

Article

# Homochiral or Heterochiral: A Systematic Study of Threonine Clusters Using a FT ICR Mass Spectrometer

Luyang Jiao<sup>1</sup>, Mengying Du<sup>1</sup>, Yameng Hou<sup>1</sup>, Yuan Ma<sup>1</sup> and Xianglei Kong<sup>1,2,\*</sup> 

<sup>1</sup> State Key Laboratory and Institute of Elemento–Organic Chemistry, College of Chemistry, Nankai University, Tianjin 300071, China; 2120200781@mail.nankai.edu.cn (L.J.); 2120200778@mail.nankai.edu.cn (M.D.); 2120210890@mail.nankai.edu.cn (Y.H.); 2120170893@mail.nankai.edu.cn (Y.M.)

<sup>2</sup> Collaborative Innovation Center of Chemical Science and Engineering (Tianjin), Nankai University, Tianjin 300071, China

\* Correspondence: kongxianglei@nankai.edu.cn; Tel.: +86-22-23509564

**Abstract:** The strong chiral preferences of some magic clusters of amino acids have attracted continually increasing interests due to their unique structures, properties and possible roles in homochirogenesis. However, how chirality can influence the generation and stability of cluster ions in a wide range of cluster sizes is still unknown for most amino acids. In this study, the preference for threonine clusters to form homochiral and heterochiral complex ions has been investigated by electrospray ionization (ESI) mass spectrometry. Abundant cluster  $[\text{Thr}_n+\text{mH}]^{m+}$  ions ( $7 \leq n \leq 78$ ,  $1 \leq m \leq 5$ ) have been observed for both samples of enantiopure (100% L) and racemic (50:50 L:D) threonine solutions. Further analyses of the spectra show that the  $[\text{Thr}_{14}+2\text{H}]^{2+}$  ion is characterized by its most outstanding homochiral preference, and  $[\text{Thr}_7+\text{H}]^+$  and  $[\text{Thr}_8+\text{H}]^+$  ions also clearly exhibit their homochiral preferences. Although most of the triply charged clusters ( $20 \leq n \leq 36$ ) are characterized by heterochiral preferences, the quadruply charged  $[\text{Thr}_n+4\text{H}]^{4+}$  ions ( $40 \leq n \leq 59$ ) have no obvious chiral preference in general. On the other hand, a weak homochiral preference exists for most of the quintuply charged ions observed in the experiment.



**Citation:** Jiao, L.; Du, M.; Hou, Y.; Ma, Y.; Kong, X. Homochiral or Heterochiral: A Systematic Study of Threonine Clusters Using a FT ICR Mass Spectrometer. *Symmetry* **2022**, *14*, 86. <https://doi.org/10.3390/sym14010086>

Academic Editor: Angela Patti

Received: 7 December 2021

Accepted: 4 January 2022

Published: 6 January 2022

**Publisher's Note:** MDPI stays neutral with regard to jurisdictional claims in published maps and institutional affiliations.



**Copyright:** © 2022 by the authors. Licensee MDPI, Basel, Switzerland. This article is an open access article distributed under the terms and conditions of the Creative Commons Attribution (CC BY) license (<https://creativecommons.org/licenses/by/4.0/>).

**Keywords:** chiral preference; threonine clusters; electrospray ionization; mass spectrometry; homochirality

## 1. Introduction

Clusters of amino acids can exhibit strong chiral preferences [1–6]. The most famous example is the protonated serine octamer, which is characterized by its high abundance in electrospray ionization (ESI) mass spectra and pronounced homochirality preference [1–4]. This magic ion has been generated in many ways and its structure and properties have been studied with different methods [7–33]. It is also found that the neutral octamer can be formed from spraying solutions [29]. Substitution reactions in the serine octamer were also observed for other amino acids, in which one or two units can be replaced by other L/D amino acids with homochiral preference [8,26–28]. These results have led to the suggestion that this cluster might have played a role in homochirogenesis [7,8,16].

In order to study the chiral preferences of cluster ions in a more systematic way, Nemes et al. performed a detailed study of the cluster formation of some natural and non-natural amino acids in the ESI process [5]. It was pointed out that the formation of amino acid clusters is a self-association process determined by various factors. Some magic clusters with a preference for homo- or heterochiral have been suggested. For example, the clusters of  $[\text{Ala}_6+\text{H}]^+$  and  $[\text{Pro}_4+\text{H}]^+$  are found to be homochiral, whereas  $[\text{Ile}_4+\text{H}]^+$  and  $[\text{Val}_4+\text{H}]^+$  are heterochiral.

For clusters with larger sizes, overlapping of the peaks makes their study difficult. To solve this problem, the techniques of ion mobility spectrometry (IMS) and mass spectrometry were combined and applied [6,10,34]. Using this method, Holliday et al. studied

the chiral preferences of proline clusters ( $2 \leq n \leq 23$ ) generated by ESI [34]. Remarkably, an oscillation in chiral preference was observed for these proline clusters. It has been found that homochiral assemblies were more favorable in ionic intensities than heterochiral assemblies for some singly and doubly protonated clusters; however, for others, it was the opposite [34]. In such a study, the IMS is very helpful; not only it can provide the information of the collision cross section of the cluster ions, but also a good separation for cluster ions with same isotopic peaks (such as  $[\text{Ser}_8+\text{H}]^+$ ,  $[\text{Ser}_{16}+2\text{H}]^{2+}$  and  $[\text{Ser}_{24}+3\text{H}]^{3+}$  that were simultaneously generated in one experiment [1].

Considering the structural similarity between threonine and serine, threonine clusters have also been studied. In addition to a substitution unit in serine octamer, threonine itself can form stable ions including protonated heptamer and octamer ions [5,21]. Nemes et al. have shown that the three cluster of threonine,  $[\text{Thr}_4+\text{H}]^+$ ,  $[\text{Thr}_7+\text{H}]^+$  and  $[\text{Thr}_{10}+\text{H}]^+$ , have homochiral preferences [5]. However, for large-sized and multiply charged threonine clusters, the relative studies are insufficient. In this study, we aimed to study how chirality can influence the cluster ions of L/D-threonine generated in the ESI process, especially for large-sized and multiply charged clusters. A Fourier-transform ion cyclotron resonance (FT ICR) mass spectrometer was applied for the experiment. To solve the problem of overlapped peaks from different clusters, simulations were applied to separate these ions using their theoretical isotope distributions. Based on this, the chiral preferences of threonine clusters were systematically studied in a wide range ( $7 \leq n \leq 78$ ). Some clusters characterized by their significant homochiral or heterochiral preferences have been identified for the first time.

## 2. Materials and Methods

A Varian IonSpec 7.0 T FT ICR mass spectrometer (Lake Forest, CA, USA) was utilized here to perform the ESI experiments. The Z Spray ESI source was applied with the probe biased at 3.6 kV.  $\text{N}_2$  was used as the cone and desolvation gas. The cone voltage was set at 23 V. For solutions containing only L- or D-threonine (Sigma; the purity of both samples is more than 98%), the samples were prepared in a concentration of 5 mmol/L in 60:38:2  $\text{H}_2\text{O}:\text{MeOH}:\text{AcOH}$ ; for racemic solutions, L- and D-amino acids were mixed on site to form solutions containing each of them in 2.5 mmol/L in the same solvent. Ions produced by ESI through a syringe with a flow rate of 2  $\mu\text{L}/\text{min}$  were injected into an open-ended cylindrical Penning trap via a quadrupole ion guide. All ESI mass spectra obtained here were in the positive ion mode. Both samples are performed under identical experimental conditions that were optimized for large-sized and multiply charged cluster ions.

## 3. Results and Discussion

Figure 1 shows the mass spectra of the pure sample of L-threonine and the racemic sample of L/D-threonine in the region of 500–2000  $m/z$ . The experiment for pure sample of D-threonine was also tried and the spectrum was very similar to that of pure L-threonine. Series of cluster ions were observed for both samples. Generally, these peaks can be clearly designated as  $[\text{Thr}_n+m\text{H}]^{m+}$  (and abbreviated to be  $n^{+m}$  in the figure), according to their charge states and sizes. Most of the observed clusters in Figure 1 are triply or quadruply charged, but some of them are singly, doubly and quintuply charged. From Figure 1, it can be concluded that the distributions of these ions generated from enantiopure and racemic solutions are basically the same, although there are still some differences.

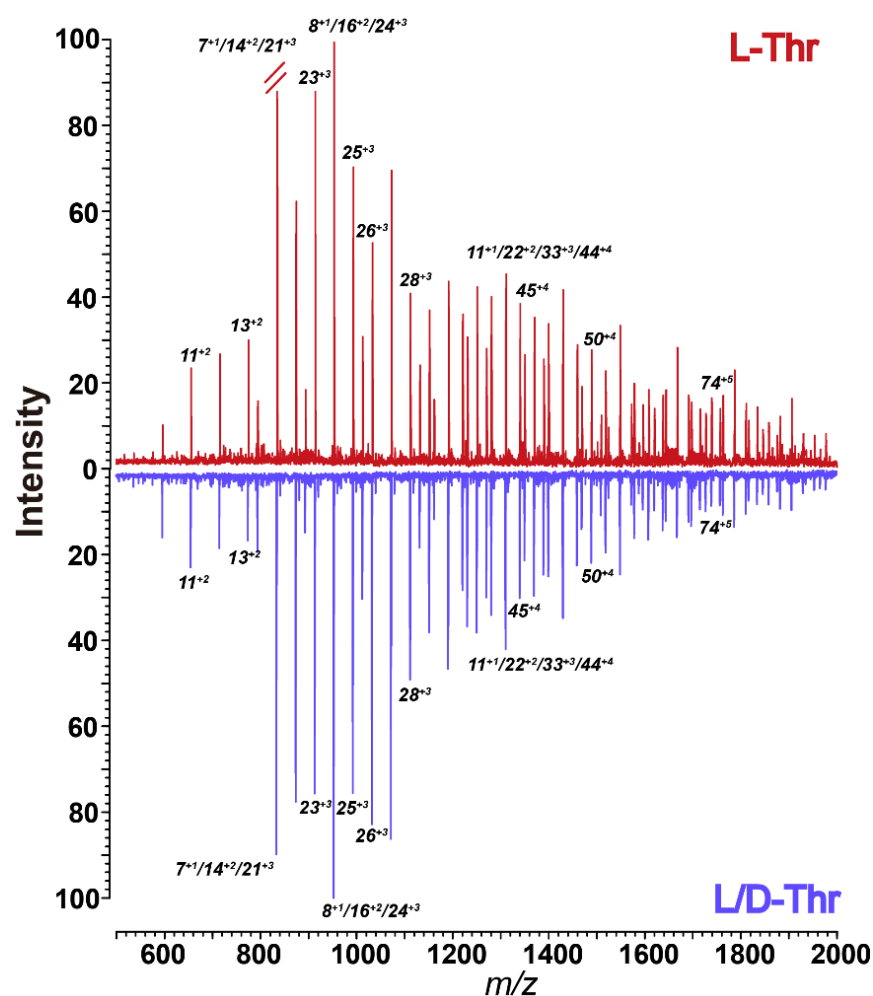


**Figure 1.** A comparison of the ESI mass spectra of enantiopure (100% L) and racemic (50:50 L:D) threonine solutions in the range of 500–2000  $m/z$ . To facilitate the comparison, their experimental peak intensities were normalized with a unified standard. Due to the very strong signal close to 834  $m/z$  for the enantiopure sample, the peaks at 834  $m/z$  have been cut off and are shown separately in Figure 2.

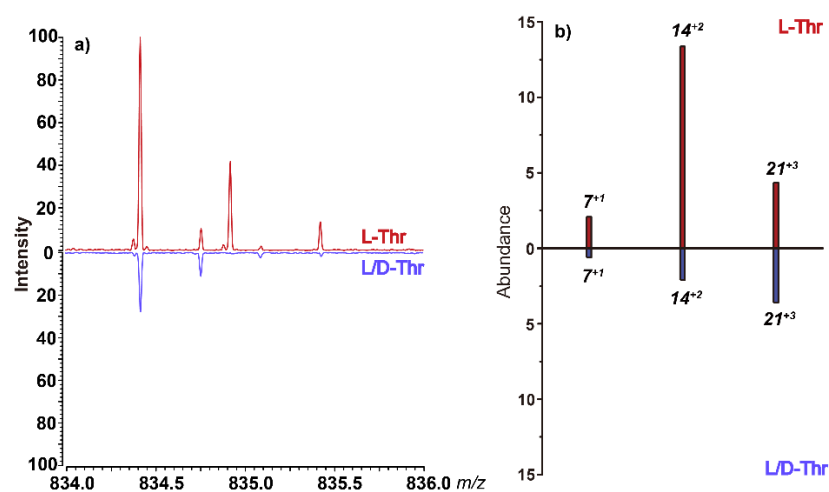


**Figure 2.** (a) The peaks close to 834  $m/z$  from the enantiopure (100% L) and racemic (50:50 L:D) threonine solutions; (b) the comparison of ions after decomposition of the mass spectra.

Considering that the enantiopure sample generated a much stronger peak at  $\sim 834$   $m/z$  (removed from Figure 1) than that of the racemic sample, the details of these peaks were checked, and the results are shown in Figure 2a. Additionally, the corresponding result of enantiopure D-threonine was also checked, which was very similar to that of enantiopure L-sample. Relying on the high resolution of the FT ICR mass spectrometer, it was found that the strong signal from L-threonine, in fact, is a combination of the three ions  $[\text{Thr}_7+\text{H}]^{1+}$ ,  $[\text{Thr}_{14}+2\text{H}]^{2+}$  and  $[\text{Thr}_{21}+3\text{H}]^{3+}$ . The three ions have the same  $m/z$  as their single natural isotope peaks, but different isotope distributions. Similar phenomena have previously been observed in the cases of serine and other amino acids. Here, using the simulation method that has been reported in our previous paper [35], the signals were decomposed into the sum of the three cluster ions. Results showed that the percentages of these three ions,  $[\text{Thr}_7+\text{H}]^{1+}$ ,  $[\text{Thr}_{14}+2\text{H}]^{2+}$  and  $[\text{Thr}_{21}+3\text{H}]^{3+}$ , were 13%, 67% and 20%, respectively. However, the simulation for signals from racemic solutions gave different results: the percentages of these three ions were 14%, 32% and 54%, respectively. The comparisons of the intensities of these three ions generated from the two solutions are listed in Figure 2b. Clearly, the intensities of  $[\text{Thr}_{21}+3\text{H}]^{3+}$  had negligible changes for both samples, whereas the intensities of  $[\text{Thr}_7+\text{H}]^{1+}$  and  $[\text{Thr}_{14}+2\text{H}]^{2+}$  had dramatically decreased from the enantiopure to the racemic samples.

The chiral preference can be calculated as:

$$C = \frac{I_L - I_r}{I_L + I_r} \quad (1)$$

where  $C$  is the chiral preference,  $I_L$  and  $I_r$  are the intensities of the corresponding ions generated from enantiopure (100% L) and racemic (50:50 L:D) threonine solutions. The preferences for homochirality and heterochirality are indicated by positive and negative values located between  $-1$  and  $1$ , respectively. The value of  $0$  indicates no chiral preference.

Based on the decomposed results, the chiral preferences of the three ions,  $[\text{Thr}_7+\text{H}]^{1+}$ ,  $[\text{Thr}_{14}+2\text{H}]^{2+}$  and  $[\text{Thr}_{21}+3\text{H}]^{3+}$  are  $0.37$ ,  $0.73$  and  $0.09$ , respectively. The results show no chiral preference for  $[\text{Thr}_{21}+3\text{H}]^{3+}$ , but a clear homochiral preference for  $[\text{Thr}_7+\text{H}]^{1+}$ , of which the latter is in good agreement with Nemes et al.'s results [5]. Remarkably, the  $[\text{Thr}_{14}+2\text{H}]^{2+}$  ion showed a very strong homochiral preference, about twice as much as that of  $[\text{Thr}_7+\text{H}]^{1+}$ .

The details shown in Figure 2 prompted us to re-analyze each peak observed in Figure 1 carefully to avoid errors. Thus, the ion peaks were not only compared with each other for both samples, but also compared with the theoretical calculated isotope distributions of the identified cluster ions or possible combinations of relative ions. The results show that for most of the observed peaks in Figure 1, their isotope distributions fit the theoretical simulations of corresponding reasonably with doubly, triply, quadruply and quintuply charged ions. The ions of  $[\text{Thr}_n+2\text{H}]^{2+}$  ( $n = 11, 13, 15, 17, 19$ ),  $[\text{Thr}_n+3\text{H}]^{3+}$  ( $n = 20, 22, 23, 25, 26, 28, 29, 31, 32, 34, 35$ ),  $[\text{Thr}_n+4\text{H}]^{4+}$  ( $n = 41-43, 45-47, 49-51, 53-55, 58, 59$ ) and  $[\text{Thr}_n+5\text{H}]^{5+}$  ( $n = 64, 66-69, 71, 73, 74, 76$ ) observed in both enantiopure and racemic samples belong to this class. For such ions, their intensities generated from the two samples can be directly compared. Figure 3 shows examples of  $[\text{Thr}_n+3\text{H}]^{3+}$  ( $n = 22, 23, 25, 26, 28, 29$ ). It can be reflected that for  $[\text{Thr}_{23}+3\text{H}]^{3+}$ , the chiral preference is close to zero, whereas for  $[\text{Thr}_{22}+3\text{H}]^{3+}$ ,  $[\text{Thr}_{26}+3\text{H}]^{3+}$  and  $[\text{Thr}_{28}+3\text{H}]^{3+}$ , the values are  $-0.36$ ,  $-0.45$  and  $-0.42$ , respectively, indicating their heterochiral preferences. Similarly, the examples of  $[\text{Thr}_n+4\text{H}]^{4+}$  ( $n = 43, 45, 46$ ) are shown in Figure 4a-c, indicating that these ions have very weak chiral preferences. However, for the larger cluster of  $[\text{Thr}_{71}+5\text{H}]^{5+}$ , a slight homochiral preference can be observed.

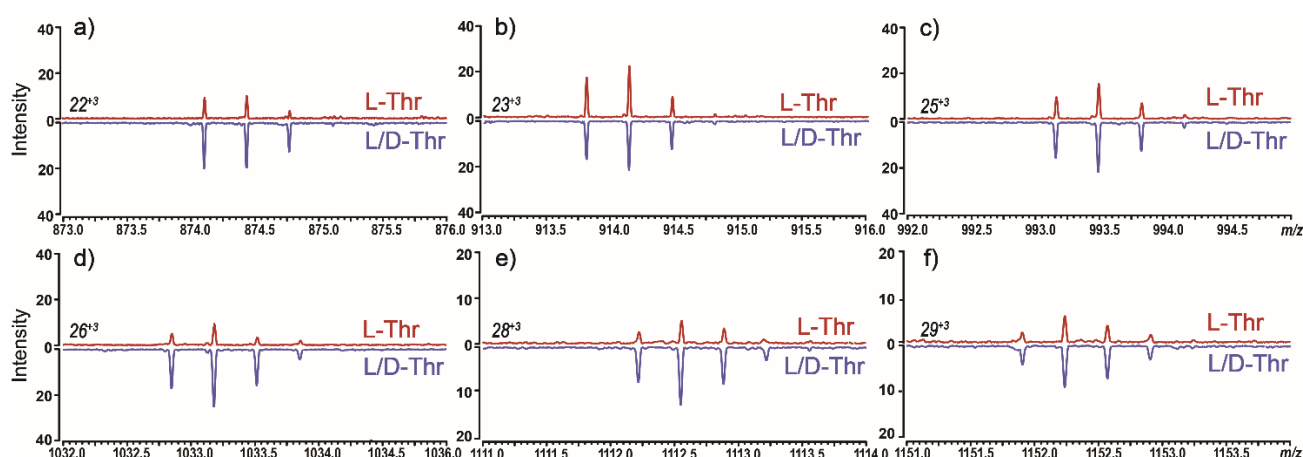


**Figure 3.** The comparisons of some threonine clusters generated from enantiopure (100% L) and racemic (50:50 L:D) solutions: (a)  $[\text{Thr}_{22}+3\text{H}]^{3+}$ , (b)  $[\text{Thr}_{23}+3\text{H}]^{3+}$ , (c)  $[\text{Thr}_{25}+3\text{H}]^{3+}$ , (d)  $[\text{Thr}_{26}+3\text{H}]^{3+}$ , (e)  $[\text{Thr}_{28}+3\text{H}]^{3+}$  and (f)  $[\text{Thr}_{29}+3\text{H}]^{3+}$ .

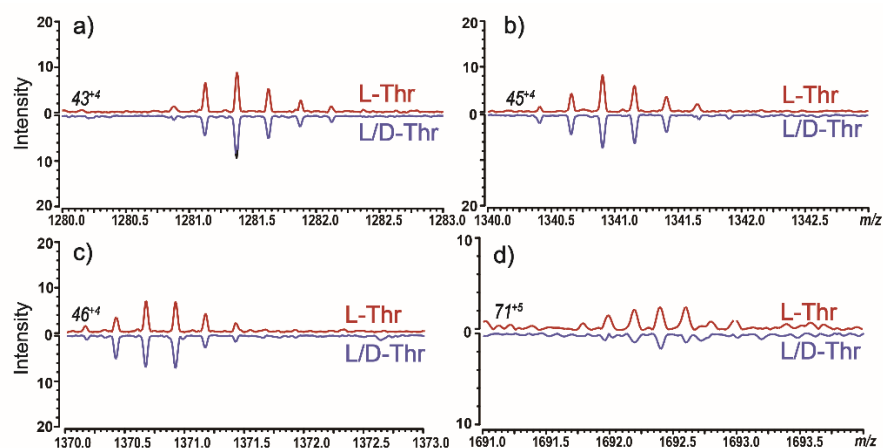


**Figure 4.** The comparisons of some threonine clusters generated from enantiopure (100% L) and racemic (50:50 L:D) solutions: (a)  $[\text{Thr}_{43}+4\text{H}]^{4+}$ , (b)  $[\text{Thr}_{45}+4\text{H}]^{4+}$ , (c)  $[\text{Thr}_{46}+4\text{H}]^{4+}$ , (d)  $[\text{Thr}_{71}+5\text{H}]^{5+}$ .

On the other hand, the clusters that had sizes as integer multiples of their corresponding charge states ( $>2$ ), such as  $[\text{Thr}_n+3\text{H}]^{3+}$  ( $n = 24, 27, 30, 33, 36$ ),  $[\text{Thr}_n+4\text{H}]^{4+}$  ( $n = 44, 48, 52, 56$ ) and  $[\text{Thr}_n+5\text{H}]^{5+}$  ( $n = 65, 70$ ), were characterized by their complex isotope distributions, indicating the co-existence of multiple ions. For example, the signals of  $[\text{Thr}_{24}+3\text{H}]^{3+}$  and  $[\text{Thr}_8+\text{H}]^{1+}$  overlapped together, along with weak signals of  $[\text{Thr}_{24}+2\text{H}]^{2+}$ , making the whole spectrum difficult to read. Using the simulation, the spectrum could be reconstructed by assuming the percentages of these three ions,  $[\text{Thr}_8+\text{H}]^{1+}$ ,  $[\text{Thr}_{16}+2\text{H}]^{2+}$  and  $[\text{Thr}_{24}+3\text{H}]^{3+}$ , as 47%, 22% and 31% for L-threonine, respectively. For the racemic sample, the three percentages were 63%, 24% and 13%, respectively. Based on the results, the chiral preferences of the three ions were calculated to be 0.45, 0.02 and 0.01, respectively, indicating a typical homochiral preference of the  $[\text{Thr}_8+\text{H}]^{1+}$  ion.

Based on the method described above, all the signals in Figure 1 have been analyzed. The chiral preference plot for all identified cluster ions is shown in Figure 5. In addition to the cluster ions mentioned above, some cluster ions with larger sizes, such as triply charged clusters with  $n > 28$ , and quadruply charged cluster ions with  $n > 56$ , were also included in the figure. The standard deviations obtained by three experiments are also shown there. In addition to the previously determined homochiral cluster of  $[\text{Thr}_7+\text{H}]^+$  [15],  $[\text{Thr}_8+\text{H}]^+$  also showed a close homochiral preferences to the former, whereas  $[\text{Thr}_{14}+2\text{H}]^{2+}$  showed the greatest homochiral preference among all observed ions in this experiment, with a value

almost twice as high as the first one. The clusters of  $[\text{Thr}_{21}+3\text{H}]^{3+}$  and  $[\text{Thr}_{26-28}+3\text{H}]^{3+}$  showed clear heterochiral preferences. An overall view of Figure 5 also shows some interesting findings. The variations in their chiral preferences of doubly charged cluster ions reflected the structures of the small-sized clusters being very sensitive to their sizes. For triply charged clusters ( $20 \leq n \leq 36$ ), insignificant heterochiral preferences are observed; however, for most of the quadruply charged cluster ions ( $40 \leq n \leq 60$ ), no obvious chiral preference was observed. On the other hand, for  $[\text{Thr}_n+5\text{H}]^{5+}$  ions ( $64 \leq n \leq 76$ ), a weak homochiral preference can be observed for most of them. The reason of the general oscillation is still unclear. This may be caused by the size of the clusters, but also may be the odd or even-numbered protons carried.

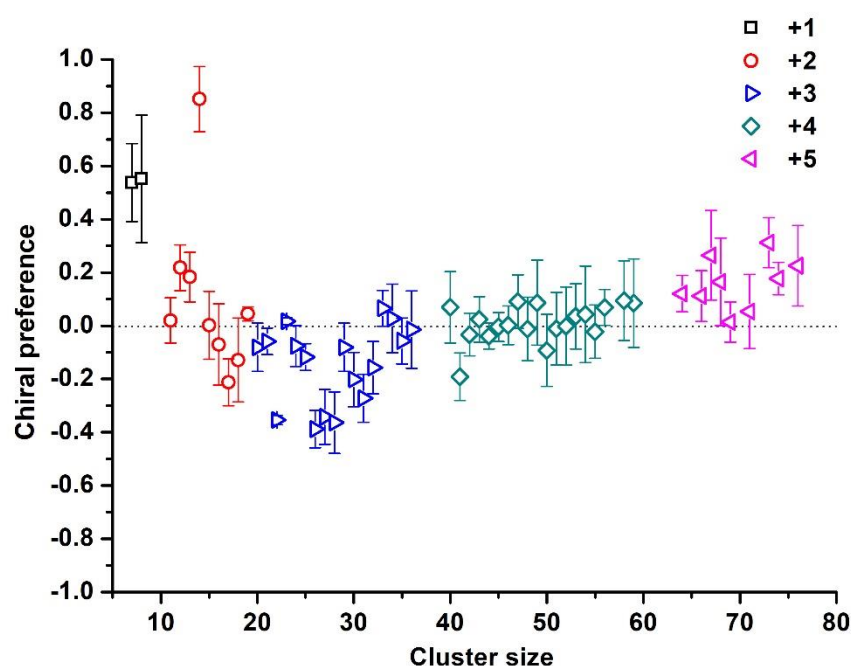


**Figure 5.** Chiral preference plot for  $[\text{Thr}_n+m\text{H}]^{m+}$  clusters. Positive and negative values indicate preferences for homochirality and heterochirality, respectively. The error bars representing the standard deviations obtained by collecting datasets in triplicates are also shown in the figure.

The results also raise questions on the formation of cluster ions in the ESI process [25,28,34]. The homochiral preference of  $[\text{Thr}_{14}+2\text{H}]^{2+}$  is almost the double of that of  $[\text{Thr}_7+\text{H}]^+$ , supporting the idea that the formation of cluster of  $[\text{Thr}_{14}+2\text{H}]^{2+}$  does proceed via the assembly of two homochiral units of  $[\text{Thr}_7+\text{H}]^+$ . However, the  $[\text{Thr}_{21}+3\text{H}]^{3+}$  ion exhibited no chiral preference, showing a different formation process or an assembly process without the need of homochirality for the assembling units. A previous study by Emily et al. suggested that the generation of a serine octamer and threonine octamer could be best explained with the ion evaporation mechanism, but that of large-sized serine/threonine clusters should be explained with the charge residue mechanism [25]. Thus, it is possible that the  $[\text{Thr}_7+\text{H}]^+$  and  $[\text{Thr}_{14}+2\text{H}]^{2+}$  ions were mainly generated through ion evaporation, whereas  $[\text{Thr}_{21}+3\text{H}]^{3+}$  was generated through the charge residue mechanism. To obtain a clearer picture of this, further well-designed experiments, including isotope substitution and varying ESI conditions, are necessary.

#### 4. Conclusions

The preference for threonine clusters to form complex homochiral and heterochiral ions has been investigated by ESI mass spectrometry. Abundant cluster ions of  $[\text{Thr}_n+m\text{H}]^{m+}$  ( $7 \leq n \leq 78$ ,  $1 \leq m \leq 5$ ) have been observed for both samples. Careful analysis of the spectra should be performed to prevent possible misinterpretation due to overlapping ion

peaks. The results showed that both  $[\text{Thr}_7+\text{H}]^+$  and  $[\text{Thr}_8+\text{H}]^+$  ions exhibit clear homochiral preferences, and the  $[\text{Thr}_{14}+2\text{H}]^{2+}$  ion showed the greatest homochiral preference among all observed ions in this experiment. Additionally, heterochiral preferences have been observed for  $[\text{Thr}_{26-28}+3\text{H}]^{3+}$ . Variations in chiral preferences have been observed for doubly charged cluster ions. Interestingly, most of the triply charged clusters ( $20 \leq n \leq 36$ ) are characterized by their insignificant heterochiral preferences. For the quadruply charged ions  $[\text{Thr}_n+4\text{H}]^{4+}$  ( $40 \leq n \leq 59$ ), no obvious chiral preference has been observed. However, for  $[\text{Thr}_n+5\text{H}]^{5+}$  ions with larger sizes ( $64 \leq n \leq 76$ ), a weak but general homochiral preference was observed. These results also provide a different perspective to understand the generation of clusters and the relationship with chirality relative to their cluster sizes.

**Author Contributions:** Conceptualization, X.K.; Experiments, Y.H., L.J., M.D. and Y.M.; Data analysis, L.J. and M.D.; writing—original draft preparation, X.K. and L.J.; writing—review and editing, X.K.; funding acquisition, X.K. All authors have read and agreed to the published version of the manuscript.

**Funding:** This research was funded by the National Natural Science Foundation of China (21627801).

**Institutional Review Board Statement:** Not applicable.

**Informed Consent Statement:** Not applicable.

**Data Availability Statement:** The data are available on request from the corresponding author.

**Conflicts of Interest:** The authors declare no conflict of interest.

## References

1. Cooks, R.G.; Zhang, D.; Koch, K.J.; Gozzo, F.C.; Eberlin, M.N. Chiroselective Self-Directed Octamerization of Serine: Implications for Homochirogenesis. *Anal. Chem.* **2001**, *73*, 3646–3655. [[CrossRef](#)] [[PubMed](#)]
2. Counterman, A.E.; Clemmer, D.E. Magic Number Clusters of Serine in the Gas Phase. *J. Phys. Chem. B* **2001**, *105*, 8092–8096. [[CrossRef](#)]
3. Hodyss, R.; Julian, R.R.; Beauchamp, J.L. Spontaneous chiral separation in noncovalent molecular clusters. *Chirality* **2001**, *13*, 703–706. [[CrossRef](#)] [[PubMed](#)]
4. Julian, R.R.; Hodyss, R.; Kinnear, B.; Jarrold, M.F.; Beauchamp, J.L. Nanocrystalline Aggregation of Serine Detected by Electrospray Ionization Mass Spectrometry: Origin of the Stable Homochiral Gas-Phase Serine Octamer. *J. Phys. Chem. B* **2002**, *106*, 1219–1228. [[CrossRef](#)]
5. Nemes, P.; Schlosser, G.; Vékey, K. Amino acid cluster formation studied by electrospray ionization mass spectrometry. *J. Mass Spectrom.* **2005**, *40*, 43–49. [[CrossRef](#)]
6. Julian, R.R.; Myung, S.; Clemmer, D.E. Spontaneous Anti-Resolution in Heterochiral Clusters of Serine. *J. Am. Chem. Soc.* **2004**, *126*, 4110–4111. [[CrossRef](#)]
7. Koch, K.J.; Gozzo, F.C.; Nanita, S.C.; Takats, Z.; Eberlin, M.N.; Cooks, R.G. Chiral Transmission between Amino Acids: Chirally Selective Amino Acid Substitution in the Serine Octamer as a Possible Step in Homochirogenesis. *Angew. Chem. Int. Ed.* **2002**, *41*, 1721–1724. [[CrossRef](#)]
8. Takats, Z.; Nanita, S.C.; Cooks, R.G. Serine Octamer Reactions: Indicators of Prebiotic Relevance. *Angew. Chem. Int. Ed.* **2003**, *42*, 3521–3523. [[CrossRef](#)]
9. Nanita, S.C.; Takats, Z.; Cooks, R.G.; Myung, S.; Clemmer, D.E. Chiral enrichment of serine via formation, dissociation, and soft-landing of octameric cluster ions. *J. Am. Soc. Mass Spectr.* **2004**, *15*, 1360–1365. [[CrossRef](#)]
10. Myung, S.; Julian, R.R.; Nanita, S.C.; Cooks, R.G.; Clemmer, D.E. Formation of Nanometer-Scale Serine Clusters by Sonic Spray. *J. Phys. Chem. B* **2004**, *108*, 6105–6111. [[CrossRef](#)]
11. Takats, Z.; Cooks, R.G. Thermal formation of serine octamer ions. *Chem. Commun.* **2004**, *4*, 444–445. [[CrossRef](#)]
12. Gronert, S.; O’Hair, R.A.J.; Fagin, A.E. Ion/molecule reactions of the protonated serine octamer. *Chem. Commun.* **2004**, *17*, 1944–1945. [[CrossRef](#)]
13. Mazurek, U.; Geller, O.; Lifshitz, C.; McFarland, M.A.; Marshall, A.G.; Reuben, B.G. Protonated Serine Octamer Cluster: Structure Elucidation by Gas-Phase H/D Exchange Reactions. *J. Phys. Chem. A* **2005**, *109*, 2107–2112. [[CrossRef](#)] [[PubMed](#)]
14. Nanita, S.C.; Cooks, R.G. Negatively-Charged Halide Adducts of Homochiral Serine Octamers. *J. Phys. Chem. B* **2005**, *109*, 4748–4753. [[CrossRef](#)] [[PubMed](#)]
15. Yang, P.; Xu, R.; Nanita, S.C.; Cooks, R.G. Thermal Formation of Homochiral Serine Clusters and Implications for the Origin of Homochirality. *J. Am. Chem. Soc.* **2006**, *128*, 17074–17086. [[CrossRef](#)] [[PubMed](#)]
16. Nanita, S.C.; Cooks, R.G. Serine Octamers: Cluster Formation, Reactions, and Implications for Biomolecule Homochirality. *Angew. Chem. Int. Ed.* **2006**, *45*, 554–569. [[CrossRef](#)]

17. Mazurek, U. Letter: Some More Aspects of Formation and Stability of the Protonated Serine Octamer Cluster. *Eur. J. Mass Spectrom.* **2006**, *12*, 63–69. [[CrossRef](#)]
18. Nanita, S.C.; Sokol, E.; Cooks, R.G. Alkali metal-cationized serine clusters studied by sonic spray ionization tandem mass spectrometry. *J. Am. Soc. Mass Spectr.* **2007**, *18*, 856–868. [[CrossRef](#)]
19. Kong, X.; Tsai, I.A.; Sabu, S.; Han, C.-C.; Lee, Y.T.; Chang, H.-C.; Tu, S.-Y.; Kung, A.H.; Wu, C.-C. Progressive Stabilization of Zwitterionic Structures in [H(Ser)<sub>2–8</sub>]<sup>+</sup> Studied by Infrared Photodissociation Spectroscopy. *Angew. Chem. Int. Ed.* **2006**, *45*, 4130–4134. [[CrossRef](#)]
20. Kong, X.; Lin, C.; Infusini, G.; Oh, H.-B.; Jiang, H.; Breuker, K.; Wu, C.-C.; Charkin, O.P.; Chang, H.-C.; McLafferty, F.W. Numerous Isomers of Serine Octamer Ions Characterized by Infrared Photodissociation Spectroscopy. *Chemphyschem A Eur. J. Chem. Phys. Phys. Chem.* **2009**, *10*, 2603–2606. [[CrossRef](#)]
21. Sunahori, F.X.; Yang, G.; Kitova, E.N.; Klassen, J.S.; Xu, Y. Chirality recognition of the protonated serine dimer and octamer by infrared multiphoton dissociation spectroscopy. *Phys. Chem. Chem. Phys.* **2013**, *15*, 1873–1886. [[CrossRef](#)]
22. Seo, J.; Warnke, S.; Pagel, K.; Bowers, M.T.; von Helden, G. Infrared spectrum and structure of the homochiral serine octamer-dichloride complex. *Nat. Chem.* **2017**, *9*, 1263–1268. [[CrossRef](#)]
23. Scutelnic, V.; Perez, M.A.S.; Marianski, M.; Warnke, S.; Gregor, A.; Rothlisberger, U.; Bowers, M.T.; Baldauf, C.; von Helden, G.; Rizzo, T.R.; et al. The Structure of the Protonated Serine Octamer. *J. Am. Chem. Soc.* **2018**, *140*, 7554–7560. [[CrossRef](#)] [[PubMed](#)]
24. Zhang, H.; Wei, Z.; Jiang, J.; Cooks, R.G. Nebulization Prior to Isolation, Ionization, and Dissociation of the Neutral Serine Octamer Allows Its Characterization. *Angew. Chem. Int. Ed.* **2018**, *57*, 17141–17145. [[CrossRef](#)]
25. Spencer, E.A.C.; Ly, T.; Julian, R.R. Formation of the serine octamer: Ion evaporation or charge residue? *Int. J. Mass Spectrom.* **2008**, *270*, 166–172. [[CrossRef](#)]
26. Liao, G.H.; Yang, Y.J.; Kong, X.L. Chirality effects on proline-substituted serine octamers revealed by infrared photodissociation spectroscopy. *Phys. Chem. Chem. Phys.* **2014**, *16*, 1554–1558. [[CrossRef](#)]
27. Ren, J.; Wang, Y.Y.; Feng, R.X.; Kong, X.L. Investigation of L/D-threonine substituted L-serine octamer ions by mass spectrometry and infrared photodissociation spectroscopy. *Chin. Chem. Lett.* **2017**, *28*, 537–540. [[CrossRef](#)]
28. Shi, Y.Y.; Zhou, M.; Zhang, K.L.; Ma, L.F.; Kong, X.L. Chiral Differentiation of Non-Covalent Diastereomers Based on Multichannel Dissociation Induced by 213-nm Ultraviolet Photodissociation. *J. Am. Soc. Mass Spectr.* **2019**, *30*, 2297–2305. [[CrossRef](#)]
29. Chen, R.; Wei, Z.; Cooks, R.G. Collection and Characterization by Mass Spectrometry of the Neutral Serine Octamer Generated upon Sublimation. *Anal. Chem.* **2021**, *93*, 1092–1099. [[CrossRef](#)]
30. Jordan, J.S.; Williams, E.R. Effects of Electrospray Droplet Size on Analyte Aggregation: Evidence for Serine Octamer in Solution. *Anal. Chem.* **2021**, *93*, 1725–1731. [[CrossRef](#)]
31. Jordan, J.S.; Williams, E.R. Dissociation of large gaseous serine clusters produces abundant protonated serine octamer. *Analyst* **2021**, *146*, 2617–2625. [[CrossRef](#)] [[PubMed](#)]
32. Jordan, J.S.; Williams, E.R. Homochiral preference of serine octamer in solution and formed by dissociation of large gaseous clusters. *Analyst* **2021**, *146*, 6822–6830. [[CrossRef](#)] [[PubMed](#)]
33. Pietrusiewicz, K.M.; Borkowski, M.; Strzelecka, D.; Kielar, K.; Kicińska, W.; Karevych, S.; Jasiński, R.; Demchuk, O.M. A General Phenomenon of Spontaneous Amplification of Optical Purity under Achiral Chromatographic Conditions. *Symmetry* **2019**, *11*, 680. [[CrossRef](#)]
34. Holliday, A.E.; Atlasevich, N.; Myung, S.; Plasencia, M.D.; Valentine, S.J.; Clemmer, D.E. Oscillations of Chiral Preference in Proline Clusters. *J. Phys. Chem. A* **2013**, *117*, 1035–1041. [[CrossRef](#)]
35. Kong, X.L. Serine-phosphoric acid cluster ions studied by electrospray ionization and tandem mass spectrometry. *J. Mass Spectrom.* **2011**, *46*, 535–545. [[CrossRef](#)]